Persistency studies of trails and silhouettes on square and triangular lattices

1989 J. Phys. A: Math. Gen. 22 3059

(http://iopscience.iop.org/0305-4470/22/15/021)

J. Phys. A: Math. Gen. 22 (1989) 3059–3079. Printed in the UK

Persistency studies of trails and silhouettes on square and triangular lattices

D E Burnette and H A Lim

Supercomputer Computations Research Institute, Florida State University, Tallahassee, FL 32306-4052, USA

Received 12 December 1988, in final form 11 April 1989

Abstract. We study the persistencies of trails and silhouettes on two-dimensional square and triangular lattices. These persistencies are induced by fixing the first step of the walk in the positive x direction. Trails are walks which are not allowed to overlap on themselves but may self-intersect whereas silhouettes are just the shadows of trails. Associated with each self-intersection is an attractive interaction energy $\varepsilon = -|\varepsilon|$. Thus a fugacity factor $(f(I,\theta) = e^{I\varepsilon/k_B T} = e^{I\theta}$, where I is the number of intersections) may be defined. This has the advantage of providing a handle on the temperature and such dependence of persistencies on temperature is studied for the first time in this paper. They are found to obey a law that may be expressed as a function of the critical exponents: $\langle X_l^{2k+1}(\theta)\rangle \sim l^{pkv(\theta)} f(l)$ where l is the chain length, v is the correlation exponent, $f(l) \sim \log_e l$ or some weak function of l (e.g. l^w where $w \ll 1.0$), p is a parameter and $k = 0, 1, 2 \ldots$.

1. Introduction

It is well known that initial perturbations imposed on some physical systems may persist to future times as the systems evolve (see, for example, [1]). Such persistency may also arise in stochastic walks on regular lattices [2–11]. For example, in random walks (RW) in which the excluded-volume constraint is neglected, the walk may be started one lattice spacing away from an excluded point [4, 7]; or in self-avoiding walks (SAW) where the excluded-volume constraint is important, the walk may be started with the initial step fixed in a certain direction [5–7]. In all these cases, persistencies of the bias of the walk distribution in the direction of the first step are the physical quantities of interest. A measure to quantify the amount of the vestiges of this bias is the persistence length which is defined as the component of the end-to-end vector in the direction of the initial step. It has been found by various independent studies [5–11] that the averaged first moment of a persistence length in the direction of the initial step may be a power law of the chain length l, while a logarithmic dependence cannot be completely ruled out. Redner and Privman pursued this problem further by studying numerically the averaged odd moments of a persistence length, and provided a scaling analysis in support of their findings [6]. Their conclusion was that the averaged first moment increases logarithmically with the chain length l and the averaged odd mth moment ($m = 2k + 1$ and $k = 1, 2, \ldots$) increases as $l^{2kv} \ln l$ ($\ln \equiv \log_e$) where v is the correlation exponent. This finding is interesting as it shows that the averaged odd moments of a persistence length may be expressed as a function of the critical exponents of the system.

0305-4470/89/153059+21$02.50

A variant of these RW and SAW model persistency studies is a partially directed self-avoiding walk in which the first step is fixed in the $+x$ direction and the subsequent steps are either in $+x$ or $\pm y$. This model has been solved analytically and the averaged first moment of the persistence length in the $+x$ direction is found to be a constant, i.e. $\langle X \rangle \to (1 + 1/\sqrt{2})$ as the number of steps tends to infinity [6]. The problem of the persistency of walk models is thus far from settled and a resolution is still needed. In this paper, we ask a similar question in the trail [12–17] and in the silhouette [8, 18] models, where the initial step is fixed in a fixed direction, $+x$ say. Trails are walks whose bonds are not allowed to overlap, but may self-intersect (see figure 1). Associated with each self-intersection, an interaction energy $\varepsilon = -|\varepsilon|$ is introduced so that a fugacity factor $f(I, \theta) = e^{I\beta\varepsilon} = e^{I\theta}$ may be defined for each walk configuration (I is the number of intersections, $\beta = 1/k_B T$). It suffices to mention that as $\theta \to -\infty$, intersections are suppressed and the usual SAW are recovered; in the limit of $\theta \to +\infty$, configurations with maximal number of intersections will dominate. It is thus obvious that this model interpolates in a non-trivial way the RW and SAW models [8, 16–18]. It is thus interesting to see how the persistency of this model would behave.

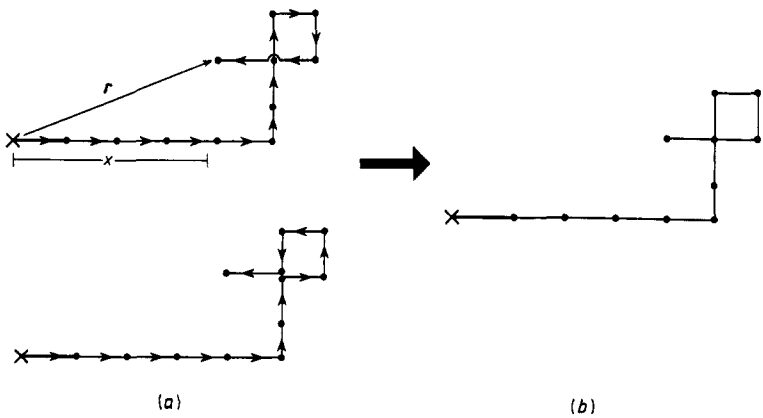

Figure 1. (*a*) Two topologically distinct trails with an intersection: a self-crossing intersection (top) and an osculating intersection (bottom). Associated with each intersection is a factor of e^{θ}; (*b*) the corresponding silhouette. The persistence length is just the x component of the end-to-end vector r.

Silhouettes [8, 18] on the other hand, are just the shadows of trails, i.e. the equivalence class of trails when the chronological order of the building bonds is ignored (see figure 1). This model is interesting in its own right for it has been shown via renormalisation group analysis [15] that it possesses non-Gaussian tricritical exponents, distinct from its Θ-point counterparts of self-attracting SAW (see [19, 20] and references therein). Exact enumeration studies have also shown that trails and silhouettes have different tricritical exponents at their respective tricritical points [8, 16–18]. Moreover, the temperature dependence (via the fugacity factor) provides a possible probe for exploring the region at which the models (trails and silhouettes) transit from their respective swollen regimes to their respective collapsed regimes as the temperature is lowered.

The study of persistencies in trails and silhouttes is interesting in another respect: we recall that on regular lattices the coordination numbers are finite. So for trails (silhouettes), any point may be visited only a finite number of times (for example, on a

square lattice, a point may be visited at most twice, except the initial point which may be visited thrice) after which the point is saturated and becomes an 'excluded point'. We thus see that the persistence length of the trail and the silhouette models may have some of the property of an excluded-point problem as well as an excluded-volume (from no bond overlap) problem. This should be constrasted with SAW in which every point traversed by the walk is immediately 'excluded' (because of no overlap and no self-intersection). Another related but noteworthy point is that for SAW, an excluded-point constraint is equivalent to fixing the direction of the first step [6, 7] whereas in trails (silhouettes), the excluded-point constraint is very different from fixing the direction of the first step since in the latter, the walk may self-intersect. Thus we see that the 'excluded-point' constraint is somewhat relaxed in the trail and the silhouette models. Consequently, we would also expect intuitively that the persistence lengths of trails and silhouettes would be smaller in magnitude than those of SAW.

It is the main purpose of this paper to investigate by exact enumeration the persistencies of trails and silhouettes on two-dimensional (2D) square (loose-packed) and triangular (close-packed) lattices. In §2, we will define the symbols and the thermodynamical functions that we will use in subsequent sections. Section 3 presents the results of exact enumerations and §4 discusses the various analysis methods of the first four averaged odd moments of the persistence lengths. In §5, the results for the square lattice are presented while the corresponding results for the triangular lattice are given in §6. In §7, comparisons of the persistencies of the two models and of the two models on the two lattices are made, and are compared and contrasted with those of SAW and 'excluded-point' RW. A conclusion of our investigation is also drawn in the same section.

2. Symbols and thermodynamic functions

If we denote by $C(l, I, r)$ the total number of trails (silhouettes) with length l, having I intersections and end-to-end distance r, then the total number of trails (silhouettes) of length l with I intersections, and the ensemble end-to-end vector $\boldsymbol{R}$ (see figure 1) are given respectively by

$$c(l, I) = \sum_{r} C(l, I, r) \tag{1a}$$

$$\boldsymbol{R}(l, I) = \sum_{r} \boldsymbol{r}(l, I, r) C(l, I, r). \tag{1b}$$

The ensemble end-to-end vector $\boldsymbol{R}$ should not be confused with the configurational end-to-end vector $\boldsymbol{r}$ which is the end-to-end vector of a particular configuration. The partition function (for configurations of length l) on a lattice is thus

$$Z_l(\theta) = \sum_{I \geq 0} c(l, I) \mathrm{e}^{I\theta}. \tag{2}$$

From equations (1*b*) and (2), the first moment of the persistence length and the averaged mth moment of the persistence length along the direction of the initial step $(+x)$ are respectively defined as [5–8]

$$X(l, I) = \boldsymbol{R}(l, I) \cdot \hat{x} = \sum_{r} x(l, I, r) C(l, I, r) \tag{3a}$$

$$\langle X_l^m(\theta)\rangle = \frac{\sum_I \sum_r x^m(l,I,r)C(l,I,r)e^{I\theta}}{Z_l(\theta)}$$

$$= \frac{\sum_I X^m(l,I)e^{I\theta}}{Z_l(\theta)} \qquad m = 1,2,3,\ldots \tag{3b}$$

where $\hat{x}$ is a unit vector in the $+x$ direction and $\langle\ldots\rangle$ denotes ensemble average of the argument.

Following [6–8], we shall now focus our attention only on the odd moments because they provide a natural way to quantify any asymmetry of the displacement distribution induced by fixing the first step. In these references, it has been shown that the averages of odd moments of persistence lengths for SAW of length l in 2D can be expressed as ($\ln \equiv \log_e$)

$$\langle X_l^{2k+1}\rangle \sim \begin{cases} \ln l & \text{if } k = 0 \\ l^{2k\nu} \ln l & \text{if } k = 1,2,\ldots. \end{cases} \tag{4}$$

It is interesting to note that the averaged first moment is of the same functional form as the analytical prediction for random walk with an excluded point [4, 7]. The question thus is whether the averaged first moment and higher odd moments of the persistence lengths of trails and silhouettes would scale according to the same law.

3. Exact enumeration

In the exact enumeration process, the first step is always fixed along the positive x direction. This serves the dual purposes of reducing enumeration time by a factor of $1/q$ where q is the coordination number (from rotational symmetry consideration of unperturbed walks) and of setting up the initial 'perturbation'—the persistency of which will be studied. We have enumerated the first four odd moments, categorised according to the number of intersections I, and the chain lengths l (see tables 1–4).

Tabulated in this manner, the averaged moments of the persistence length may be studied as a function of temperature via the fugacity factor $f(I,\theta) = e^{I\theta}$ (and/or as a function of the chain length). It might be argued that our chains are relatively short ($l = 20$ for square lattice and $l = 13$ for triangular lattice), but it should be noted that we have classified the data into different topological classes according to the number of intersections. In fact, the crux of the enumeration lies in this classification which takes up most of the memory and consumes the major part of the computer runtime. This is especially true when there is no general topological relation(s) relating the number of trails to the corresponding number of silhouettes. All the enumerations take about 30 CPU hours on a VAX 8700.

3.1. Square lattice

On this lattice, the enumeration is performed with the $\hat{x}$ and $\hat{y}$ axes as the basis vectors. Since the first link is fixed along the positive x direction, the configurational mth moment persistence length is simply the mth power of the component of the configurational end-to-end vector r along the x direction, i.e. $(r \cdot \hat{x})^m$. Table 1 presents the first three odd moments of the persistence length, $X^{2k+1}(l,I)$ $(k = 0,1,2)$ for trails of chain length up to $l = 20$ and number of intersections of $I = 6$; table 2 gives the

Table 1. Trails on a square lattice: (*a*) the first odd moment of the persistence length $X(l, I)$; (*b*) the second odd moment of the persistence length $X^3(l, I)$; (*c*) the third odd moment of the persistence length $X^5(l, I)$. Notation: E$N \equiv \times 10^N$.

l	$I=0$	$I=1$	$I=2$	$I=3$	$I=4$	$I=5$	$I=6$
(*a*)	$X(l, I)$						
3	0.13000E2						
4	0.40000E2	0.00000E0					
5	0.11700E3	0.20000E1					
6	0.33800E3	0.12000E2					
7	0.95500E3	0.58000E2	0.20000E1				
8	0.26880E4	0.22000E3	0.16000E2				
9	0.74650E4	0.81000E3	0.74000E2				
10	0.20698E5	0.27160E4	0.33600E3	0.80000E1			
11	0.56901E5	0.90020E4	0.12280E4	0.84000E2			
12	0.15627E6	0.28508E5	0.45600E4	0.38400E3			
13	0.42669E6	0.89274E5	0.15490E5	0.18040E4	0.40000E2		
14	0.11642E7	0.27294E6	0.52268E5	0.68320E4	0.46400E3		
15	0.31632E7	0.82605E6	0.17042E6	0.25780E5	0.22200E4		
16	0.85897E7	0.24645E7	0.54671E6	0.91512E5	0.10544E5	0.20800E3	
17	0.23252E8	0.72931E7	0.17263E7	0.31382E6	0.41504E5	0.24640E4	
18	0.62918E8	0.21375E8	0.53748E7	0.10568E7	0.15714E6	0.13120E5	0.16000E3
19	0.16983E9	0.62246E8	0.16559E8	0.34655E7	0.56945E6	0.60800E5	0.24000E4
20	0.45824E9	0.18001E9	0.50481E8	0.11218E8	0.19971E7	0.25514E6	0.18208E5
(*b*)	$X^3(l, I)$						
3	0.61000E2						
4	0.29200E3	0.00000E0					
5	0.12210E4	0.20000E1					
6	0.46880E4	0.24000E2					
7	0.16951E5	0.22600E3	0.20000E1				
8	0.58704E5	0.13960E4	0.64000E2				
9	0.19666E6	0.73380E4	0.43400E3				
10	0.64197E6	0.33724E5	0.26040E4	0.80000E1			
11	0.20522E7	0.14281E6	0.12772E5	0.25200E3			
12	0.64482E7	0.56667E6	0.58536E5	0.18240E4			
13	0.19971E8	0.21430E7	0.24834E6	0.12412E5	0.23200E3		
14	0.61102E8	0.77980E7	0.10035E7	0.65416E5	0.33440E4		
15	0.18499E9	0.27508E8	0.38913E7	0.31671E6	0.19692E5		
16	0.55497E9	0.94581E8	0.14583E8	0.14094E7	0.11062E6	0.83200E3	
17	0.16516E10	0.31827E9	0.53155E8	0.59020E7	0.53144E6	0.15376E5	
18	0.48808E10	0.10515E10	0.18913E9	0.23631E8	0.24061E7	0.10202E6	0.16000E3
19	0.14333E11	0.34198E10	0.65923E9	0.91093E8	0.10292E8	0.61640E6	0.14784E5
20	0.41853E11	0.10970E11	0.22569E10	0.34056E9	0.42192E8	0.31541E7	0.16134E6
(*c*)	$X^5(l, I)$						
3	0.37300E3						
4	0.27400E4	0.00000E0					
5	0.16077E5	0.20000E1					
6	0.81608E5	0.72000E2					
7	0.37446E6	0.11380E4	0.20000E1				
8	0.15948E7	0.11380E5	0.25600E3				
9	0.64158E7	0.85050E5	0.35540E4				
10	0.24671E8	0.52688E6	0.29916E5	0.80000E1			
11	0.91470E8	0.28604E7	0.19743E6	0.92400E3			
12	0.32906E9	0.14094E8	0.11264E7	0.10944E5			
13	0.11542E10	0.64454E8	0.58065E7	0.11196E6	0.10000E4		
14	0.39623E10	0.27794E9	0.27781E8	0.82871E6	0.29264E5		
15	0.13353E11	0.11428E10	0.12548E9	0.52403E7	0.24846E6		
16	0.44278E11	0.45178E10	0.54087E9	0.29288E8	0.17589E7	0.33280E4	
17	0.14476E12	0.17281E11	0.22431E10	0.14956E9	0.10440E8	0.11502E6	
18	0.46742E12	0.64268E11	0.90022E10	0.71241E9	0.56269E8	0.10336E7	0.16000E3
19	0.14925E13	0.23331E12	0.35123E11	0.32105E10	0.28133E9	0.84346E7	0.12000E6
20	0.47183E13	0.82939E12	0.13370E12	0.13826E11	0.13286E10	0.54852E8	0.20548E7

Table 2. Silhouettes on a square lattice: (*a*) the first odd moment of the persistence length $X(l, I)$; (*b*) the second odd moment of the persistence length $X^3(l, I)$; (*c*) the third odd moment of the persistence length $X^5(l, I)$.

l	$I = 0$	$I = 1$	$I = 2$	$I = 3$	$I = 4$	$I = 5$	$I = 6$
(*a*)	$X(l, I)$						
3	0.13000E2						
4	0.40000E2	0.00000E0					
5	0.11700E3	0.10000E1					
6	0.33800E3	0.60000E1					
7	0.95500E3	0.29000E2	0.33333E0				
8	0.26880E4	0.11000E3	0.26667E1				
9	0.74650E4	0.40500E3	0.12667E2				
10	0.20698E5	0.13580E4	0.59333E2	0.50000E0			
11	0.56901E5	0.45010E4	0.22300E3	0.55833E1			
12	0.15627E6	0.14254E5	0.84467E3	0.26500E2			
13	0.42669E6	0.44637E5	0.29310E4	0.12583E3	0.87273E0		
14	0.11642E7	0.13647E6	0.10041E5	0.49150E3	0.11300E2		
15	0.31632E7	0.41303E6	0.33290E5	0.18823E4	0.58350E2		
16	0.85897E7	0.12323E7	0.10812E6	0.68203E4	0.28271E3	0.17810E1	
17	0.23252E8	0.36466E7	0.34560E6	0.23753E5	0.11471E4	0.23032E2	
18	0.62918E8	0.10687E8	0.10883E7	0.81345E5	0.44332E4	0.13310E3	0.52632E0
19	0.16983E9	0.31123E8	0.33885E7	0.27088E6	0.16414E5	0.63429E3	0.78417E1
20	0.45824E9	0.90003E8	0.10421E8	0.88962E6	0.58679E5	0.27490E4	0.63045E2
(*b*)	$X^3(l, I)$						
3	0.61000E2						
4	0.29200E3	0.00000E0					
5	0.12210E4	0.10000E1					
6	0.46880E4	0.12000E2					
7	0.16951E5	0.11300E3	0.33333E0				
8	0.58704E5	0.69800E3	0.10667E2				
9	0.19666E6	0.36690E4	0.72667E2				
10	0.64197E6	0.16862E5	0.43933E3	0.50000E0			
11	0.20522E7	0.71407E5	0.21970E4	0.16083E2			
12	0.64482E7	0.28333E6	0.10269E5	0.12400E3			
13	0.19971E8	0.10715E7	0.44497E5	0.85233E3	0.52364E1		
14	0.61102E8	0.38990E7	0.18341E6	0.45645E4	0.76755E2		
15	0.18499E9	0.13754E8	0.72481E6	0.22456E5	0.46865E3		
16	0.55497E9	0.47291E8	0.27636E7	0.10159E6	0.27118E4	0.71238E1	
17	0.16516E10	0.15914E9	0.10236E8	0.43269E6	0.13470E5	0.14053E3	
18	0.48808E10	0.52577E9	0.36951E8	0.17615E7	0.62716E5	0.99665E3	0.52632E0
19	0.14333E11	0.17099E10	0.13052E9	0.69034E7	0.27584E6	0.61107E4	0.46726E2
20	0.41853E11	0.54851E10	0.45224E9	0.26223E8	0.11605E7	0.32060E5	0.52955E3
(*c*)	$X^5(l, I)$						
3	0.37300E3						
4	0.27400E4	0.00000E0					
5	0.16077E5	0.10000E1					
6	0.81608E5	0.36000E2					
7	0.37446E6	0.56900E3	0.33333E0				
8	0.15948E7	0.56900E4	0.42667E2				
9	0.64158E7	0.42525E5	0.59267E3				
10	0.24671E8	0.26344E6	0.49993E4	0.50000E0			
11	0.91470E8	0.14302E7	0.33213E5	0.58083E2			
12	0.32906E9	0.70468E7	0.19168E6	0.72400E3			
13	0.11542E10	0.32227E8	0.10021E7	0.76283E4	0.22691E2		
14	0.39623E10	0.13897E9	0.48725E7	0.57267E5	0.66585E3		
15	0.13353E11	0.57141E9	0.22382E8	0.36748E6	0.57280E4		
16	0.44278E11	0.22589E10	0.98131E8	0.20812E7	0.41245E5	0.28495E2	
17	0.14476E12	0.86403E10	0.41378E9	0.10774E8	0.25086E6	0.10237E4	
18	0.46742E12	0.32134E11	0.16873E10	0.52037E8	0.13868E7	0.98779E4	0.52632E0
19	0.14925E13	0.11666E12	0.66827E10	0.23783E9	0.71179E7	0.82071E5	0.37622E3
20	0.47183E13	0.41469E12	0.25800E11	0.10388E10	0.34511E8	0.54378E6	0.65341E4

corresponding moments for silhouettes. The numbers shown are measured in units in which the lattice spacing is of length unity.

Table 3. Trails on a triangular lattice: (*a*) the first odd moment of the persistence length $X(l, I)$; (*b*) the second odd moment of the persistence length $X^3(l, I)$; (*c*) the third odd moment of the persistence length $X^5(l, I)$.

l	$I = 0$	$I = 1$	$I = 2$	$I = 3$	$I = 4$	$I = 5$	$I = 6$
(*a*)	$X(l, I)$						
2	0.60000E1						
3	0.31000E2	0.00000E0					
4	0.14900E3	0.50000E1					
5	0.69000E3	0.60000E2	0.40000E1				
6	0.31260E4	0.46100E3	0.62000E2				
7	0.13953E5	0.29520E4	0.57400E3	0.80000E1			
8	0.61618E5	0.17118E5	0.42520E4	0.26200E3			
9	0.26995E6	0.93267E5	0.27614E5	0.32520E4	0.84000E2		
10	0.11754E7	0.48684E6	0.16549E6	0.28068E5	0.19040E4		
11	0.50924E7	0.24626E7	0.93951E6	0.20372E6	0.24600E5	0.38800E3	
12	0.21974E8	0.12162E8	0.51286E7	0.13316E7	0.22863E6	0.11728E5	
13	0.94503E8	0.58946E8	0.27169E8	0.81250E7	0.17530E7	0.16607E6	0.29840E4
(*b*)	$X^3(l, I)$						
2	0.15000E2						
3	0.13900E3	0.00000E0					
4	0.10303E4	0.57500E1					
5	0.67238E4	0.14700E3	0.25000E1				
6	0.40407E5	0.19588E4	0.14450E3				
7	0.22925E6	0.19160E5	0.22810E4	0.80000E1			
8	0.12466E7	0.15633E6	0.24568E5	0.54250E3			
9	0.65631E7	0.11314E7	0.21744E6	0.11190E5	0.18900E3		
10	0.33680E8	0.75246E7	0.17000E7	0.14368E6	0.65300E4		
11	0.16930E9	0.47003E8	0.12189E8	0.14430E7	0.11213E6	0.65500E3	
12	0.83661E9	0.27976E9	0.81882E8	0.12454E8	0.13676E7	0.34816E5	
13	0.40756E10	0.16026E10	0.52275E9	0.96819E8	0.13562E8	0.73263E6	0.92300E4
(*c*)	$X^5(l, I)$						
2	0.47250E2						
3	0.79600E3	0.00000E0					
4	0.90506E4	0.59375E1					
5	0.82610E5	0.46125E3	0.21250E1				
6	0.65468E6	0.11033E5	0.42013E3				
7	0.47004E7	0.16413E6	0.12323E5	0.80000E1			
8	0.31375E8	0.18634E7	0.20041E6	0.16926E4			
9	0.19802E9	0.17736E8	0.24291E7	0.55670E5	0.42525E3		
10	0.11955E10	0.14907E9	0.24571E8	0.10509E7	0.30787E5		
11	0.69629E10	0.11424E10	0.21952E9	0.14527E8	0.76464E6	0.21618E4	
12	0.39364E11	0.81512E10	0.17896E10	0.16415E9	0.12434E8	0.16107E6	
13	0.21704E12	0.54953E11	0.13588E11	0.16095E10	0.15838E9	0.47695E7	0.38692E5

3.2. Triangular lattice

On this lattice, the enumeration is performed with $\hat{x}$ and $(-1\hat{x} + \sqrt{3}\hat{y})/2$ as the basis vectors. Since the basis vectors are not orthogonal, care has to be taken so that the contributions from $(-1\hat{x} + \sqrt{3}\hat{y})/2$ are accounted for. Table 3 gives the first three odd moments of the persistence length for trails and table 4 gives the corresponding

moments for silhouettes. These numbers are also in units of unit lattice spacing. Even though the enumerations here are only up to a chain length of $l = 13$, the maximum number of intersections reached is $I = 6$, the same as the enumerations on a square lattice. Since equation (3) is essentially a series in $e^{I\theta}$, this means that we have reached the same number of terms in the expansion on both the square and the triangular lattice.

Table 4. Silhouettes on a triangular lattice: (*a*) the first odd moment of the persistence length $X(l, I)$; (*b*) the second odd moment of the persistence length $X^3(l, I)$; (*c*) the third odd moment of the persistence length $X^5(l, I)$.

l	$I = 0$	$I = 1$	$I = 2$	$I = 3$	$I = 4$	$I = 5$	$I = 6$
(*a*)	X(l,I)						
2	0.60000E1						
3	0.31000E2	0.00000E0					
4	0.14900E3	0.25000E1					
5	0.69000E3	0.30000E2	0.66666E0				
6	0.31260E4	0.23050E3	0.10333E2				
7	0.13953E5	0.14760E4	0.97250E2	0.50000E0			
8	0.61618E5	0.85590E4	0.74592E3	0.16750E2			
9	0.26995E6	0.46634E5	0.50109E4	0.21142E3	0.19091E1		
10	0.11754E7	0.24342E6	0.30908E5	0.18791E4	0.42752E2		
11	0.50924E7	0.12313E7	0.17977E6	0.14137E5	0.56959E3	0.23375E1	
12	0.21974E8	0.60811E7	0.10018E7	0.95628E5	0.55365E4	0.81458E2	
13	0.94503E8	0.29473E8	0.54019E7	0.60179E6	0.44370E5	0.12653E4	0.63128E1
(*b*)	$X^3(l, I)$						
2	0.15000E2						
3	0.13900E3	0.00000E0					
4	0.10303E4	0.28750E1					
5	0.67238E4	0.73500E2	0.41666E0				
6	0.40407E5	0.97938E3	0.24083E2				
7	0.22925E6	0.95798E4	0.38294E3	0.50000E0			
8	0.12466E7	0.78164E5	0.41914E4	0.34188E2			
9	0.65631E7	0.56569E6	0.37957E5	0.71460E3	0.42954E1		
10	0.33680E8	0.37623E7	0.30426E6	0.94393E4	0.14657E3		
11	0.16930E9	0.23501E8	0.22355E7	0.97689E5	0.25261E4	0.49281E1	
12	0.83661E9	0.13988E9	0.15365E8	0.86805E6	0.31773E5	0.25837E3	
13	0.40756E10	0.80128E9	0.10015E9	0.69405E7	0.32764E6	0.56417E4	0.22334E2
(*c*)	$X^5(l, I)$						
2	0.47250E2						
3	0.79600E3	0.00000E0					
4	0.90506E4	0.29688E1					
5	0.82610E5	0.23063E3	0.35417E0				
6	0.65468E6	0.55166E4	0.70021E2				
7	0.47004E7	0.82064E5	0.20569E4	0.50000E0			
8	0.31375E8	0.93172E6	0.33710E5	0.10605E3			
9	0.19802E9	0.88681E7	0.41442E6	0.35248E4	0.96648E1		
10	0.11955E10	0.74537E8	0.42707E7	0.68081E5	0.69276E3		
11	0.69629E10	0.57118E9	0.38959E8	0.96612E6	0.17138E5	0.17576E2	
12	0.39364E11	0.40756E10	0.32446E9	0.11206E8	0.28361E6	0.12606E4	
13	0.21704E12	0.27477E11	0.25154E10	0.11271E9	0.37185E7	0.37368E5	0.10049E3

3.3. Confidence in the enumeration

As with any calculations of this nature, where the configurations are enumerated exactly, evidence must be adduced that no configurations have been duplicated or omitted. Checks are made in several ways.

(i) We compare our numbers in the $I = 0$ column (i.e. no intersections) against the numbers for SAW in the existing literature [5, 6].

(ii) Graphs for low orders are also enumerated by hand to double check the numbers.

(iii) Where symmetries are employed in the enumeration, we have also enumerated without symmetry consideration and then symmetry consideration is used to enumerate to higher orders.

(iv) The sum of all configurations over I for a fixed l is the number of Malakis trails ($f(I, \theta) = 1$). This provides a further check against the existing literature [12, 13].

Exact agreement (wherever comparison is possible) is found in each case. This gives us confidence that our numbers are reliable and good.

3.4. Some inferences

From the way tables 1–4 are presented, careful observations or simple calculations will immediately lead to a few quick inferences. Since the tables are tabulated in this way for the first time, a few (somewhat detailed) remarks that are of general interest are in order at this point.

(i) The $I = 0$ columns in the trail and silhouettes tables are identical because in this case, trails and silhouettes are one and the same and are actually SAW.

(ii) In the $I = 1$ column, the numbers in the silhouette tables are half those in the trail tables because for configurations with one intersection, two trails have one common silhouette (see figure 1). If we recall that persistence lengths are just the arithmetic sums of the components of the configurational end-to-end vectors along the direction of the first step, we easily see that this is actually the case. There is however, no apparent simple topological relation between the number of trails having the same silhouette for higher I.

(iii) Higher-averaged moments increase at a much faster rate. Indeed, the reduced moment [6, 8] is

$$\bar{M}_l^{2k+1}(\theta) = \frac{\langle X_l^{2k+1}(\theta)\rangle}{\langle X_l^{2r+1}(\theta)\rangle^{(2k+1)/(2r+1)}} \geq 1 \qquad \forall\, r < k. \tag{5}$$

Futhermore, $\bar{M}_l^{2k+1}(\theta)$ increases as θ increases, in accordance with previous observations [21].

(iv) $\langle X_l^{2k+1}(\theta)\rangle$ decreases as θ increases because the configurations are more compact as θ increases.

(v) It is also interesting to note the behaviour of the ratio $r(l, I) = X(l, I)/c(l, I)$. With the exception of a few $r(l, I)$ (configurations with maximal number of intersections) which show 'anomalous' behaviour, $r(l, I)$ increases as l increases for a fixed I; $r(l, I)$ decreases as I increases for a fixed l. The 'anomalies' are easily explained. Without loss of generality, we will explain the 'anomaly' observed in $(l, I) = (9, 2)$. Configuration $(7, 2)$ corresponds to figure 2. As the chain length increases, the persistency does not increase at a rate as fast as the increase in $c(l, I)$, and hence the observed 'dip' in $r(9, 2)$. Other anomalies are similarly explained but they are expected to vanish as $l \to \infty$.

(vi) It is also worth noting that $X(I) = \sum_l X(l, I)/\sum_l c(l, I)$ decreases as I increases. This is accounted for as a consequence of the rapid collapse of the configurations as θ is increased.

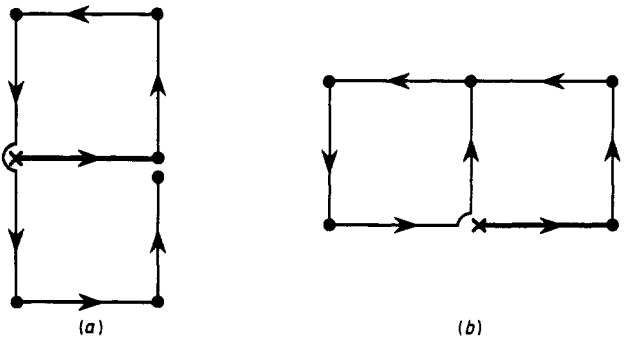

Figure 2. Two representative trails of length $l = 7$ with the maximal number of intersections. By fixing the first bond along the $+x$ direction, there are six of this type of configuration (two of (*a*) and four of (*b*)).

4. Analysis of the data

Even though there is still no consensus as to what functional form the first moment of the persistence length should be, there is a general agreement (at least by heuristic arguments) that the higher odd moments of the persistence length should scale as some power of the chain length l. It is rather unfortunate that our short exact enumeration series can provide no resolution to this controversy. We thus propose to overcome this dilemma by assuming *a priori* that the odd moments of the persistence lengths obey scaling laws of the form [5–8]:

$$\langle X_l^{2k+1}(\theta)\rangle = \begin{cases} A_0(\theta) f(l) & \text{if } k = 0 \\ A_k(\theta) l^{pk\nu(\theta)} f(l) & \text{if } k = 1, 2, \ldots \end{cases} \tag{6}$$

where the arguments show explicitly any possible temperature dependence of the various quantities, and where we have introduced a parameter p, $f(l)$ is some function of l (e.g. $f(l) \equiv \ln l$ or $f(l) \equiv l^w$ where w is an exponent) and the $A_k(\theta)$ are the amplitudes. $\nu(\theta)$ is a universal exponent and is expected to assume only three possible values [8, 16–18]:

$$\nu(\theta) = \begin{cases} \nu_{\mathrm{SAW}} & \text{if } \theta < \theta_t \quad \text{swollen phase} \\ \nu_t & \text{if } \theta = \theta_t \quad \text{tricritical point} \\ 1/d & \text{if } \theta > \theta_t \quad \text{collapsed phase} \end{cases} \tag{7}$$

where d is the dimensionality, the subscript 't' stands for 'tricritical'. If we recall that universality class is lattice independent, we would then expect persistency to be a long-range effect and thus we would also expect persistence lengths on these two lattices (square and triangular) to scale according to the same functional form. These moments of persistence lengths are best displayed by taking the Naperian logarithms of equation (6):

$$\log_{10}\langle X_l^{2k+1}(\theta)\rangle = pk\nu(\theta)\log_{10} l + \log_{10} f(l) + \log_{10} A_k. \tag{8}$$

An alternative to equation (8) is to analyse one of the reduced moments,

$$M_l^{2k+1} = \frac{\langle X_l^{2k+1}(\theta)\rangle}{\langle X_l(\theta)\rangle} = \frac{A_k l^{pk\nu(\theta)}}{A_0}. \tag{9}$$

The latter expression has the advantage that the $f(l)$ terms all drop out when a Naperian logarithm is taken.

Another useful piece of information may be extracted if we recall that trails and silhouettes [8, 16–18] share the same critical exponents except possibly at the tricritical points (of trails and silhouettes which are not necessarily one and the same). We would then expect the persistence lengths of trails and silhouettes to be equal except in the vicinity of the tricritical points. In order to facilitate comparison of trails and silhouettes, we shall highlight this by defining the differences of averaged moments of persistence lengths:

$$\begin{aligned}\Delta_l^{2k+1}(\theta) &= \langle X_l^{2k+1}(\theta)\rangle_{\text{silh}} - \langle X_l^{2k+1}(\theta)\rangle_{\text{trail}} \\ &= \left(A_k l^{pkv(\theta)} f(l)\right)_{\text{silh}} - \left(A_k l^{pkv(\theta)} f(l)\right)_{\text{trail}}.\end{aligned} \tag{10}$$

Thus, we shall analyse the persistency on each lattice in three steps:

(1) the variation of persistence length with chain length,
(2) the dependence of persistence length on temperature, and finally
(3) the variation of Δ_l^{2k+1} with temperature.

5. Analysis for trails and silhouettes on a square lattice

5.1. Variation with chain length

Figures 3 and 4 are plots of $\log_{10}\langle X_l^{2k+1}\rangle$ against $\log_{10} l$. It is obvious from the log–log plot of $\langle X\rangle$ against l that it is concave inwards towards the l axis. One may be tempted to conclude immediately that our results for the first odd moment fit $\langle X\rangle \sim \ln l$ better. However, one has to exercise caution when one is dealing with short chains ($l \sim 20$). For short chains, stiffness of the chain will tend to increase the persistence length. This may explain the relatively higher gradients of the log–log plots for low values of l. We thus decide to try to perform a least-squares fit of our data between $6 \leq l \leq 20$, but our results are not conclusive enough to discern a $\ln l$ dependence from a l^w dependence.

Log–log plots of the higher odd moments of the persistence lengths are linear for sufficiently low θ, indicating that the $f(l)$ term increases much slower than the power term. This has the important implication that $f(l)$ may be $\ln l$ or if $f(l) \sim l^w$, then $w \ll 1.0$. In fact, the latter observation is in agreement with previous simulation results that $w \sim 10^{-2}$ [5, 10]. Thus in our analysis, we will try to fit our data using a functional form

$$y = ax + b \tag{11}$$

where the slope a and the intercept b of the logarithmic plots are to be determined using a linear regression technique, i.e.

$$a = \left(\sum_{l=m}^{m+n} x_l y_l - \frac{1}{n+1}\sum_{l=m}^{m+n} y_l \sum_{l=m}^{m+n} x_l\right)\left[\sum_{l=m}^{m+n} x_l^2 - \frac{1}{n+1}\left(\sum_{l=m}^{m+n} x_l\right)^2\right]^{-1} \tag{12a}$$

$$b = \frac{1}{n+1}\left(\sum_{l=m}^{m+n} y_l - b\sum_{l=m}^{m+n} x_l\right) \tag{12b}$$

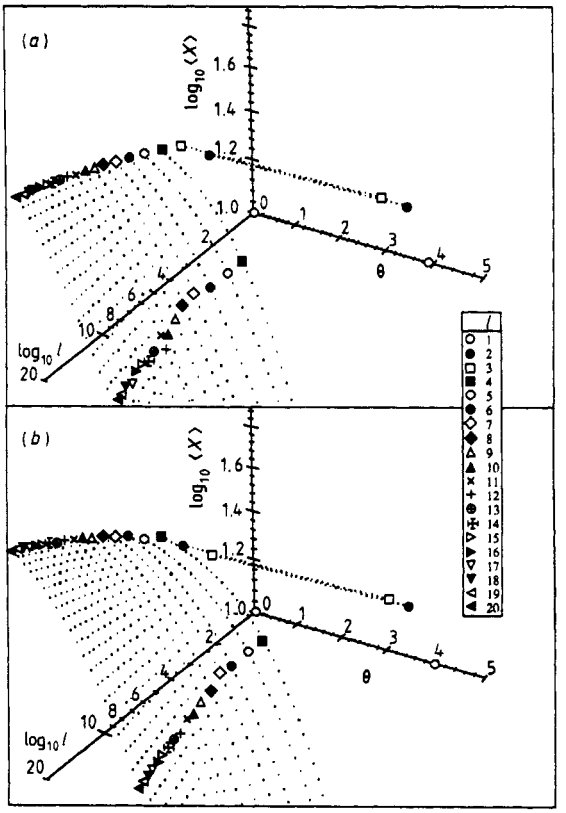

Figure 3. (*a*) A 3D plot of the first odd moment of the persistence length of trails on a square lattice as a function of the chain length l and the temperature θ. (*b*) The corresponding 3D plot for silhouettes on a square lattice.

We have best-fitted the reduced moments as defined in equation (9) by this regression technique. It should be emphasised that the regression coefficients are determined by averaging values of the coefficients obtained for $l_{\min} \leq l \leq l_{\max}$ (inclusive) where $l_{\max} = 20$ and $l_{\min} = 8, \ldots, 12$. We choose $l_{\min} \geq 8$ so that any possible stiffness of short chains is removed; and $l_{\min} \leq 12$ so that there are enough data points to fit the regression. The results are tabulated in table 5.

5.2. *Variation with temperature*

Figures 5(*a*) and 5(*b*) are the projections of figures similar to that of figure 3 onto the surfaces of constant l (l = 15–20) for the seventh moments of the persistence length ($\langle X^7 \rangle$). The other odd moments behave in a qualitatively similar manner. It is seen that as the temperature is lowered (or $\theta = 1/k_B T$ is increased), the odd moments of the persistence length decrease rather slowly at first (in the swollen regime) and then decrease very rapidly to the collapse regime within a relatively narrow range of temperature. It is not surprising that the temperature at which this rapid decrease occurs coincides closely with the tricritical temperature [9, 11]. Comparison of figures 5(*a*) and 5(*b*) reveals that for silhouettes, the collapse occurs at a larger value of θ. This would imply that the tricritical temperature of silhouettes is lower than that of

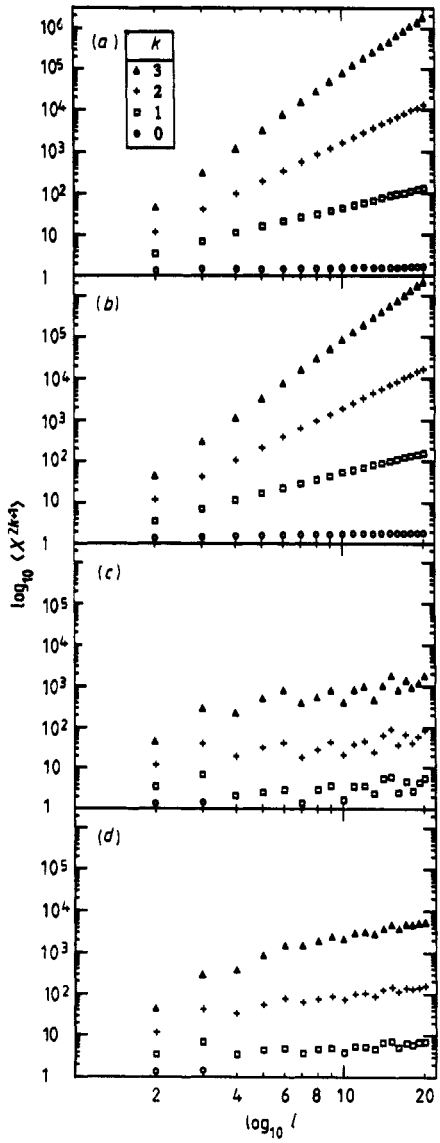

Figure 4. Log–log plots of $\langle X\rangle$, $\langle X^3\rangle$, $\langle X^5\rangle$ and $\langle X^7\rangle$ against l at a constant $\theta = 0.0$ in (*a*) trails and (*b*) silhouettes on a square lattice; and at a constant $\theta = 4.0$ in (*c*) trails and (*d*) silhouettes on a square lattice.

trails, in agreement with earlier observations [17, 18].

In table 5(*a*), we present the values of *pkv* from the best fit of equation (9) as a function of θ. We have also carefully scanned the regions in the vicinities of the tricritical temperature. In particular, at $\theta = -\infty$ (i.e. SAW), we have

$$pkv = \begin{cases} 1.557 & \text{if } k = 1 \\ 3.110 & \text{if } k = 2 \\ 4.656 & \text{if } k = 3 \end{cases} \tag{13}$$

Table 5. The values of (*a*) the linear regression coefficients of the Naperian logarithm, *pkv*, and (*b*) the prefactors, $\log_{10}(A_k/A_0)$, for the first four odd moments of the persistence lengths for trails and silhouettes on a square lattice.

	Trails			Silhouettes		
θ	$k=1$	$k=2$	$k=3$	$k=1$	$k=2$	$k=3$
(*a*) *pkv*						
$-\infty$	1.557	3.110	4.656	1.557	3.110	4.656
−5.0	1.557	3.109	4.655	1.557	3.109	4.656
−4.0	1.556	3.107	4.652	1.556	3.108	4.654
−3.0	1.553	3.102	4.645	1.555	3.106	4.651
−2.0	1.547	3.088	4.626	1.552	3.099	4.642
−1.0	1.528	3.050	4.572	1.543	3.081	4.616
0.0	1.468	2.933	4.409	1.519	3.031	4.544
1.0	1.235	2.513	3.847	1.445	2.884	4.339
1.084	1.197	2.447	3.759	1.434	2.863	4.310
1.086	1.196	2.445	3.756	1.433	2.862	4.309
1.088	1.195	2.443	3.754	1.433	2.862	4.308
1.400	1.023	2.135	3.342	1.380	2.761	4.169
2.0	0.637	1.365	2.248	1.199	2.428	3.714
2.400	0.484	0.950	1.542	1.002	2.065	3.216
3.0	0.479	0.761	0.991	0.670	1.390	2.230
4.0	0.627	1.075	1.223	0.512	0.855	1.138
5.0	0.661	1.356	1.729	0.626	1.098	1.298

	Trails				Silhouettes			
θ	$\log_{10} A_0$	$k=1$	$k=2$	$k=3$	$\log_{10} A_0$	$k=1$	$k=2$	$k=3$
(*b*) $\log_{10} A_k/A_0$								
$-\infty$	0.149	−0.065	−0.032	0.071	0.149	−0.065	−0.032	0.071
−5.0	0.149	−0.064	−0.032	0.072	0.149	−0.064	−0.032	0.071
−4.0	0.149	−0.064	−0.030	0.074	0.149	−0.064	−0.031	0.072
−3.0	0.148	−0.063	−0.027	0.079	0.149	−0.064	−0.030	0.075
−2.0	0.148	−0.059	−0.018	0.094	0.148	−0.062	−0.025	0.082
−1.0	0.146	−0.049	−0.009	0.135	0.147	−0.057	−0.013	0.102
0.0	0.147	−0.012	0.094	0.262	0.146	−0.044	0.022	0.156
1.0	0.158	0.155	0.422	0.725	0.153	−0.001	0.126	0.315
1.084	0.156	0.183	0.476	0.799	0.155	0.006	0.141	0.338
1.086	0.156	0.184	0.477	0.801	0.155	0.006	0.142	0.338
1.088	0.156	0.185	0.479	0.803	0.155	0.006	0.142	0.339
1.400	0.143	0.317	0.730	1.152	0.163	0.040	0.216	0.449
2.0	0.040	0.586	1.330	2.055	0.174	0.164	0.469	0.815
2.400	−0.057	0.636	1.579	2.567	0.149	0.304	0.749	1.219
3.0	−0.170	0.479	1.469	2.736	0.014	0.515	1.238	1.991
4.0	−0.236	0.140	0.723	1.855	−0.243	0.421	1.323	2.509
5.0	−0.229	0.008	0.174	0.882	−0.322	0.127	0.673	1.736

which, after inserting $\nu(\mathrm{SAW}) = 0.75$, leads immediately to

$$p = \begin{cases} 2.076 & \text{if } k = 1 \\ 2.073 & \text{if } k = 2 \\ 2.069 & \text{if } k = 3. \end{cases} \tag{14}$$

These results are in excellent agreement with the result of $p = 2.0$ obtained from scaling analysis [6]. Similarly for $\theta = 0$ (Malakis trails), we have

$$pkv = \begin{cases} 1.468 & \text{if } k = 1 \\ 2.933 & \text{if } k = 2 \\ 4.409 & \text{if } k = 3 \end{cases} \tag{15}$$

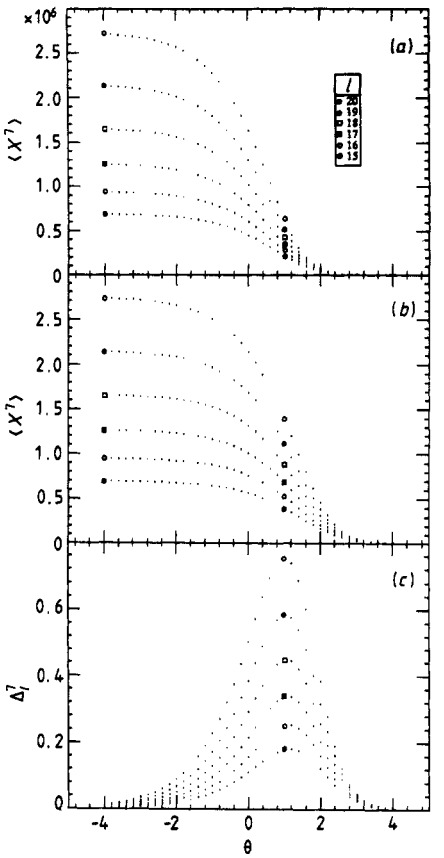

Figure 5. Plots of $\langle X^7 \rangle$ against θ for $l = 15$–20 in (a) trails and (b) silhouettes on a square lattice; and (c) a plot of Δ_l^7 for $l = 15$–20.

or that ν(Malakis) $= 0.734 \pm 0.025$ where the error bar is determined from the difference in values of ν obtained by using $p = 2.0$ and $p = 2.073$. This result is interesting as it purports the belief that Malakis trails and SAW share the same critical exponent $\nu = 0.75$. It is also very interesting to note that the values of ν extracted by this technique at $\theta = 1.088$ and 1.400 (for trails) and at $\theta = 2.4$ (for silhouettes) agree with results obtained by the scanning method [11] and by Dlog Padé approximant analysis [17, 18]. For completeness, we give in table 5(b) the estimates of the values of the prefactors A_k (see equations (6) and (9)). In the swollen phase, $A_k \sim 1.5$ whereas in the compact phase, the A_k behave more erratically.

5.3. Variation of Δ_l^{2k+1} with temperature

Figure 5(c) depicts a plot of Δ_l^7 (being representative of Δ_l^{2k+1}) against θ ($15 \leq l \leq 20$). As θ is increased from $-\infty$ to $+\infty$, Δ_l^{2k+1} increases from zero, attains a maximum and then decreases back to zero. The two tails are easily explained: for $\theta < \theta_t$ (swollen phase), trails and silhouettes have the same critical exponent of 3/4 whereas for $\theta > \theta_t$, they share the same exponent of $1/d = 1/2$. Consequently, Δ_l^{2k+1} tend to a vanishing value in these regions (see equation (10)). In close propinquity to the tricritical temperatures, the moments of the persistence lengths need not be the same

and thus the non-vanishing value of Δ_l^{2k+1}. The slight skewness of the plots of Δ_l^{2k+1} is a reflection of the slightly steeper collapse of silhouettes than that of trails in the proximity of the tricritical temperatures.

6. Analysis for trails and silhouettes on a triangular lattice

We perform analyses of the odd moments of the persistence lengths of trails and silhouettes on a triangular lattice in parallel to the analyses of the odd moments of the persistence lengths of trails and silhouettes on a square lattice. This will make comparisons of the results from these two lattices more transparent.

6.1. Variation with chain length

Figures 6 and 7 illustrate the plots of $\log_{10}\langle X_l^{2k+1}\rangle$ against $\log_{10} l$. Again, we observe the linear behaviour of the plots for sufficiently low θ (i.e. before the transition region). The regression coefficients, tabulated in table 6(*a*), are extracted from $l_{\min} \leq l \leq l_{\max}$ (inclusive) where $l_{\min} = 5, \ldots, 9$ while $l_{\max}$ is held fixed at 13. The qualitative behaviours are quite similar to those observed for trails and silhouettes on a square lattice and we shall not elaborate further.

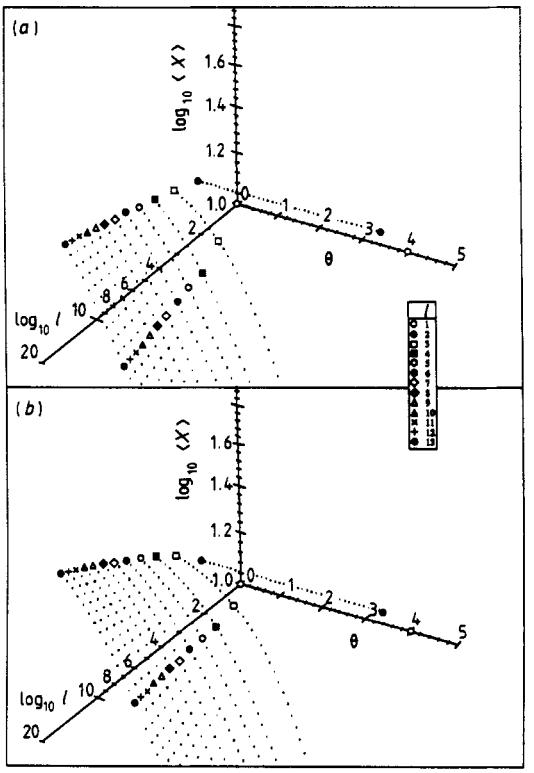

Figure 6. A 3D plot of the first odd moment of the persistence length of (*a*) trails and (*b*) silhouettes on a triangular lattice as a function of the chain length l and the temperature θ.

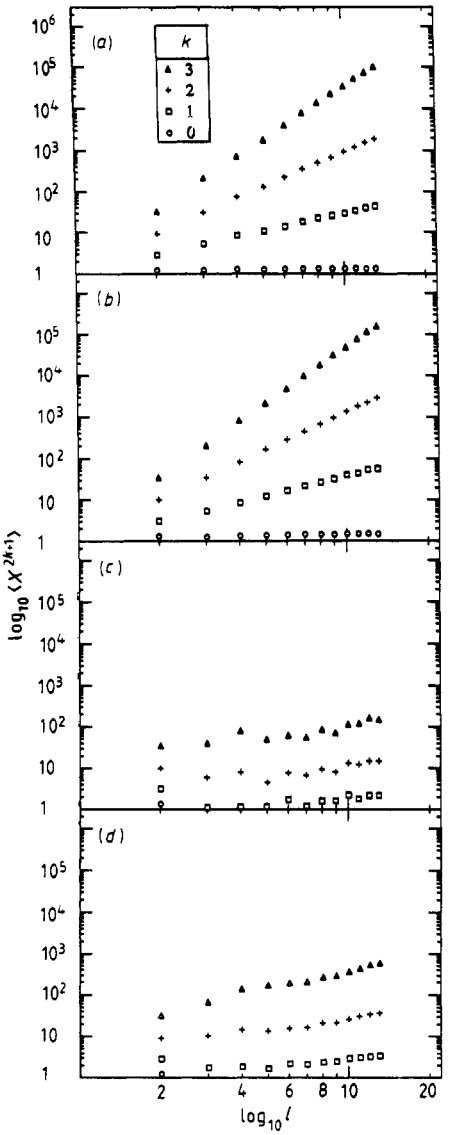

Figure 7. Log–log plots of $\langle X\rangle$, $\langle X^3\rangle$, $\langle X^5\rangle$ and $\langle X^7\rangle$ against l at a constant $\theta = 0.0$ in (*a*) trails and (*b*) silhouettes on a triangular lattice; and at a constant $\theta = 4.0$ in (*c*) trails and (*d*) silhouettes on a triangular lattice.

6.2. Variation with temperature

Figures 8(*a*) and 8(*b*) are slices of figures similar to that of figure 6 along surfaces of constant l (l = 8–13) for the seventh moment of the persistence length ($\langle X^7\rangle$). As the temperature is lowered, the odd moments of the persistence lengths decrease rather slowly in the swollen regime, and then decrease very rapidly in the transition region. The transition region is at a lower value of θ ($\theta \sim 0.6$) than previously observed in §5.2. This observation provides more corroboration for earlier exact enumeration studies

Table 6. The values of (*a*) the linear regression coefficients of the Naperian logarithm and (*b*) the prefactors for the first four odd moments of the persistence lengths for trails and silhouettes on a triangular lattice.

	Trails			Silhouettes		
θ	$k=1$	$k=2$	$k=3$	$k=1$	$k=2$	$k=3$
(*a*) *pkv*						
$-\infty$	1.559	3.100	4.637	1.559	3.100	4.637
−5.0	1.558	3.098	4.634	1.558	3.099	4.635
−4.0	1.556	3.094	4.629	1.557	3.097	4.633
−3.0	1.550	3.084	4.615	1.554	3.092	4.626
−2.0	1.535	3.056	4.578	1.547	3.079	4.608
−1.0	1.492	2.976	4.470	1.528	3.042	4.558
0.0	1.352	2.727	4.140	1.472	2.939	4.420
0.6	1.153	2.373	3.671	1.398	2.803	4.236
1.0	0.955	2.010	3.179	1.317	2.654	4.035
1.6	0.645	1.375	2.247	1.129	2.305	3.556
2.0	0.521	1.047	1.678	0.963	1.986	3.105
3.0	0.541	0.919	1.171	0.642	1.240	1.891
4.0	0.679	1.250	1.585	0.692	1.196	1.552
5.0	0.772	1.573	2.140	0.866	1.564	2.005

	Trails				Silhouettes			
θ	$\log_{10} A_0$	$k=1$	$k=2$	$k=3$	$\log_{10} A_0$	$k=1$	$k=2$	$k=3$
(*b*) $\log_{10} A_k/A_0$								
$-\infty$	0.083	−0.101	−0.092	−0.015	0.083	−0.101	−0.092	−0.015
−5.0	0.083	−0.101	−0.091	−0.013	0.083	−0.101	−0.092	−0.014
−4.0	0.083	−0.100	−0.089	−0.010	0.083	−0.101	−0.091	−0.012
−3.0	0.082	−0.097	−0.083	−0.001	0.083	−0.099	−0.088	−0.008
−2.0	0.080	−0.090	−0.066	0.023	0.082	−0.096	−0.080	0.004
−1.0	0.078	−0.066	−0.017	0.094	0.080	−0.086	−0.058	0.036
0.0	0.076	0.013	0.141	0.315	0.077	−0.057	0.005	0.126
0.6	0.073	0.132	0.370	0.634	0.077	−0.018	0.088	0.246
1.0	0.056	0.247	0.601	0.967	0.076	0.026	0.179	0.377
1.6	−0.016	0.394	0.964	1.554	0.064	0.127	0.389	0.687
2.0	−0.082	0.404	1.083	1.842	0.034	0.209	0.572	0.970
3.0	−0.218	0.151	0.737	1.654	−0.142	0.271	0.859	1.579
4.0	−0.288	−0.131	0.084	0.722	−0.295	0.004	0.462	1.267
5.0	−0.320	−0.309	−0.441	−0.181	−0.371	−0.304	−0.210	0.322

[16–18]. From tables 6(*a*), we get at $\theta = -\infty$

$$pkv = \begin{cases} 1.559 & \text{if } k = 1 \\ 3.100 & \text{if } k = 2 \\ 4.637 & \text{if } k = 3 \end{cases} \tag{16}$$

which, upon substituting $\nu(\text{SAW}) = 0.75$, yields

$$p = \begin{cases} 2.079 & \text{if } k = 1 \\ 2.067 & \text{if } k = 2 \\ 2.061 & \text{if } k = 3. \end{cases} \tag{17}$$

These results are again in excellent agreement with the scaling analysis result of $p = 2.0$ [6]. Similarly for $\theta = 0$ (Malakis trails), we have

$$pkv = \begin{cases} 1.352 & \text{if } k = 1 \\ 2.727 & \text{if } k = 2 \\ 4.140 & \text{if } k = 3. \end{cases} \tag{18}$$

or that ν(Malakis) $= 0.685 \pm 0.025$ where the error bar is fixed by using $p = 2.00$ and $p = 2.07$. This value of ν is smaller than the expected value of $\nu = 0.75$ from universality class consideration. This discrepancy is understandable and may be easily explained. Upon closer scrutiny of the plot of figure 8, we see that the transition temperature ($\theta \sim 0.6$) is rather close to $\theta = 0.0$ and we see thus that the moments of the persistence lengths have already begun to decrease at $\theta = 0.0$. This will also explain why the corresponding values of ν for the (Malakis) silhouettes are larger because in the latter, the transition temperature is at a larger value of θ ($\theta \sim 1.6$):

$$pk\nu = \begin{cases} 1.472 & \text{if } k = 1 \\ 2.939 & \text{if } k = 2 \\ 4.420 & \text{if } k = 3. \end{cases} \tag{19}$$

or that $\nu = 0.735 \pm 0.025$. This result is in agreement with the universality class picture. In table 6(b) are tabulated the values of A_k. In the swollen phase, $A_k \sim 1.0$ while in the collapsed phase, the A_k are more erratic.

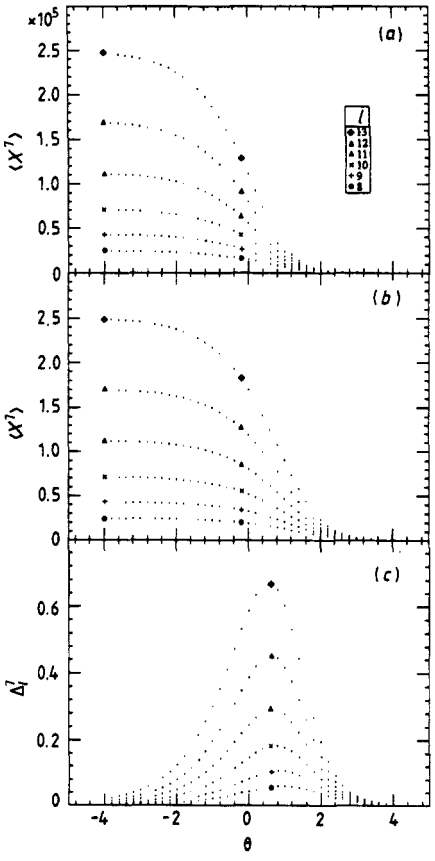

Figure 8. Plots of $\langle X^7 \rangle$ against θ for $l = 8$–13 in (a) trails and (b) silhouettes on a triangular lattice; (c) a plot of Δ_l^7 for $l = 8$–13.

6.3. *Variation of* Δ_l^{2k+1} *with temperature*

The variation of Δ_l^7 for $8 \leq l \leq 13$ as a function θ is shown in figure 8(c). The same

qualitative behaviour seen in §5.3 is also seen here, and the same explanation still holds here.

7. Discussions and conclusion

We have studied the first four odd moments of the persistence lengths of trails and silhouettes on both a square and a triangular lattice. The results from the two lattices seem to purport the universality class picture that the correlation exponent ν is lattice independent, except possibly at the tricritical points. The results also support the scaling analysis formulae that

$$\langle X_l^{2k+1}(\theta)\rangle \sim l^{pk\nu(\theta)} f(l) \tag{20}$$

where we have introduced the temperature dependence for the first time. To detect the presence of $f(l)$, we have also performed linear regressions on equation (8) (rather than equation (9)) and in each case, we find that the regression coefficients $pk\nu$ are always larger than those obtained from the Naperian logarithm of equation (9). This may be taken as an indication of the positive contributions from the $f(l)$ factor. The presence of $f(l)$ also implies that trails and silhouettes in 2D scale as SAW in 2D.

The persistence lengths of trails and silhouettes on a triangular lattice (for a fixed l) are always smaller than the corresponding persistence lengths on a square lattice. This is intuitively correct if one recalls that on a triangular lattice, the coordination number is $q = 6$ so that the bonds have more flexibility (orientations of successive bonds can be more acute or more obtuse instead of the orthogonal relative orientation on a square lattice). This is not in contradiction with the universality class picture because these differences in persistence lengths on the two lattices are absorbed not into the $l^{pk\nu}$ factor, but into the prefactors, A_k. A comparison of tables 5(b) and 6(b) would show that this is indeed the case, with the A_k on the triangular lattice smaller than those on the square lattice. This same geometrical feature also explains the lower value of transition θ on a triangular lattice because in this case nearest neighbours are more abundant and their attractive interactions tend to energetically favour collapse configurations. If we further recall that for a silhouette, there is a mutiplicity of trails, then the same energetical favouritism explanation also accounts for the observation that on a particular lattice, trails always have a lower transition θ than their silhouettes.

Probably the most important inferences we can draw from these studies are that the moments of the persistence lengths transit from the swollen phase to the compact phase within a narrow region of θ and that as the chain l increases, this region of θ narrows. If one may extrapolate this to larger l, we may then conclude that above the transition region, all walks have the same correlation exponents and likewise below the transition region—a conjecture in agreement with that of equation (7).

Acknowledgments

The authors are grateful to Mr Kenneth A Garnto and Mr Douglas S Lee for computing assistance during various stages of the project, and Dr H Meirovitch for discussions. The authors also thank the Supercomputer Computations Research Institute for the

use of the computer facilities. This work is partially supported by the US Department of Energy under the contract No DE-FC05-85ER250000.

References

[1] Adler B J and Wainwright T E 1970 *Phys. Rev.* A **1** 18
[2] Fisher M E and Sykes M F 1959 *Phys. Rev.* **114** 45
[3] Yamakawa H 1971 *Modern Theory of Polymer Solutions* (New York: Harper and Row)
[4] Weiss G H 1981 *J. Math. Phys.* **22** 562
[5] Grassberger P 1982 *Phys. Lett.* **89A** 381
[6] Redner S and Privman V 1987 *J. Phys. A: Math. Gen.* **20** L857
[7] Considine D and Redner S 1989 *J. Phys. A: Math. Gen.* **22** 1621
[8] Lim H A 1988 *J. Phys. A: Math. Gen.* **21** 3783
[9] Meirovitch H and Lim H A 1988 *Phys. Rev.* A **38** 1670
[10] Lim H A and Meirovitch H 1989 *Phys. Rev.* A **39** 4176
[11] Meirovitch H and Lim H A 1989 *Phys. Rev.* A **39** 4186
[12] Malakis A 1975 *J. Phys. A: Math. Gen.* **8** 1885
[13] Malakis A 1976 *J. Phys. A: Math. Gen.* **9** 1283
[14] Massih A R and Moore M A 1975 *J. Phys. A: Math. Gen.* **8** 237
[15] Shapir Y and Oono Y 1984 *J. Phys. A: Math. Gen.* **17** L39
[16] Lim H A, Guha A and Shapir Y 1988 *J. Phys. A: Math. Gen.* **21** 773
[17] Guha A, Lim H A and Shapir Y 1988 *J. Phys. A: Math. Gen.* **21** 1043
[18] Lim H A, Guha A and Shapir Y 1988 *Phys. Rev.* A **38** 3710
[19] Privman V 1986 *J. Phys. A: Math. Gen.* **19** 3287
[20] Duplantier B and Saleur H 1987 *Phys. Rev. Lett.* **59** 539
[21] Rapaport D C 1977 *J. Phys. A: Math. Gen.* **10** 637